JOURNAL OF AGRICULTURAL AND FOOD CHEMISTRY

Article

pubs.acs.org/JAFC

Plant Esterase−Chitosan/Gold Nanoparticles−Graphene Nanosheet Composite-Based Biosensor for the Ultrasensitive Detection of Organophosphate Pesticides

Jing Bao,[†] Changjun Hou,[*,†] Mei Chen,[†] Junjie Li,[†] Danqun Huo,[†] Mei Yang,[†] Xiaogang Luo,[†] and Yu Lei[*,§]

[†]Key Laboratory of Biorheological Science and Technology (Chongqing University), Ministry of Education, Bioengineering College, Chongqing University, Chongqing 400030, China

[§]Department of Chemical and Biomolecular Engineering, University of Connecticut, 191 Auditorium Road, Unit 3222, Storrs, Connecticut 06269, United States

Supporting Information

ABSTRACT: As broad-spectrum pesticides, organophosphates (OPs) are widely used in agriculture all over the world. However, due to their neurotoxicity in humans and their increasing occurrence in the environment, there is growing interest in their sensitive and selective detection. This paper reports a new cost-effective plant esterase−chitosan/gold nanoparticles−graphene nanosheet (PLaE-CS/AuNPs-GNs) biosensor for the sensitive detection of methyl parathion and malathion. Highly pure plant esterase is produced from plants at low cost and shares the same inhibition mechanism with OPs as acetylcholinesterase, and then it was used to prepare PLaE-CS/AuNPs-GNs nanocomposites, which were systematically characterized using SEM, TEM, and UV−vis. The PLaE-CS/AuNPs-GNs composite-based biosensor measured as low as 50 ppt (0.19 nM) of methyl parathion and 0.5 ppb (1.51 nM) of malathion (S/N = 3) with a calibration curve up to 200 ppb (760 nM) and 500 ppb (1513.5 nM) for methyl parathion and malathion, respectively. There is also no interference observed from most of common species such as metal ions, inorganic ions, glucose, and citric acid. In addition, its applicability to OPs-contaminated real samples (carrot and apple) was also demonstrated with excellent response recovery. The developed simple, sensitive, and reliable PLaE-CS/AuNPs-GNs composite-based biosensor holds great potential in OPs detection for food and environmental safety.

KEYWORDS: *plant esterase, gold nanoparticles, graphene nanosheets, organophosphates, biosensor*

INTRODUCTION

Due to their wide spectrum of insecticidal activity, organophosphorus pesticides (OPs) account for 38% of the total pesticides applied in crop protection all over the world.[1,2] Although the use of pesticides can enhance the yield of agricultural industry, it also poses huge threats to the environment, public health, and food safety.[3,4] OPs irreversibly inhibit the activity of acetylcholinesterase (AChE), which interferes with the function of vital organs and eventually causes respiratory paralysis and death.[5,6] Therefore, the development of a rapid, accurate, sensitive, reliable, and low-cost pesticide detection method is highly demanded to secure our food and environmental safety.

As OPs are extremely toxic, the U.S. Environmental Protection Agency (EPA) sets very low maximum contaminant levels (MCLs) for them, for example, 2 ppb for methyl parathion and 140 ppb for malathion in drinking water. Consequently, their detection requires ultrasensitive biosensors. As AChE is a biorecognition element highly sensitive to the inhibition of organophosphates, carbamate pesticides, and nerve gases, AChE-based biosensors for OPs have been extensively investigated in past decades.[7,9] However, both the high cost and lesser accessibility (extracted from animal blood or tissue[10]) of AChE greatly limit its wide application. Recently, as an alternative of AChE, plant esterase (EC 3.1.1.*X*) has received much attention because plant esterase and AChE share a similar sensitivity and inhibition mechanism with OP pesticides. Moreover, plant esterase can be extracted from a number of plants such as wheat, soybean, rice, and sorghum at low cost and with easy obtainment,[10−12] thus holding great potential in OPs detection. In this study, the ultrasensitive and irreversible inhibition of plant esterase activity by OPs will be first exploited to develop a simple, sensitive, and accurate plant esterase biosensor to detect OP pesticides.[13−15]

To improve the biosensor performance, various nanomaterials with high electrical conductivity, high surface to volume ratio, retention of biological activities, and good chemical and mechanical stability have been employed to enhance the electrochemical signal and the stability of AChE biosensors, such as SnO_2NPs/carboxylic graphene,[8] AuNPs/MWCNTs,[16] AuNPs/PB[17] MWCNTs/gold nanocomposites,[18] ZrO_2/CHIT composite film,[19] TiO_2-decorated graphene,[20] and CdS-decorated graphene nanocomposite.[21] Particularly, gold nanoparticles (AuNPs) and graphene nanosheets (GNs) gained extensive attention in electrocatalysis and biosensing applications. Recently, AuNPs have been widely utilized in a number of studies to detect proteins, metal ions, nucleic acids, and

Received: August 18, 2015
Revised: October 25, 2015
Accepted: November 10, 2015

DOI: 10.1021/acs.jafc.5b03971
J. Agric. Food Chem. XXXX, XXX, XXX−XXX

organic molecules owing to its good electron transfer property, large surface area, and desirable biocompatibility.[22−24] In conjunction with high-cost AChE, AuNPs are also used in the development of AChE-based biosensors.[25−28] However, due to the noncontinuity of immobilized AuNPs, further enhancement of electrical conductivity is required to develop electrochemical biosensors with high performance.[29−31] In this regard, graphene nanosheets are excellent candidates due to their excellent conductivity, mechanical properties, and high surface areas. Furthermore, chitosan (CS) is a nontoxic natural hydrophilic polysaccharide and can entangle with enzyme and nanomaterials, thus providing a favorable microenvironment to enzymes in biosensor applications, due to its good adhesion, good biocompatibility, and excellent film-forming ability.[32−34]

Herein we report a new plant esterase-based biosensor by taking synergistic advantages of chitosan, gold nanoparticles, and graphene nanosheets to accomplish ultrasensitive and selective detection of OPs. The central hypothesis is that plant esterase possesses high sensitivity to the inhibition of organophosphates, similar to AChE, whereas the nanostructured CS/AuNPs-GNs hybrid nanocomposite would promote electron transfer, enhance electric conductivity, and also provide a favorable microenvironment for enzyme in OPs detection. The as-prepared nanocomposite biosensor was systematically characterized using scanning electron microscopy (SEM), transmission electron microscopy (TEM), and cyclic voltammetry (CV). Under optimal conditions, ultrasensitive detection of methyl parathion and malathion was realized through differential pulse voltammetry (DPV) with good selectivity. The successful application of the as-developed biosensor for the detection of organophosphorus pesticides spiked in carrots and apples further demonstrates its applicability in real sample detection.

EXPERIMENTAL PROCEDURES

Reagents and Materials. The plant esterase (PLaE 129.2 U/mL) was prepared according to a method reported elsewhere.[10] 1-Naphthyl acetate (1-NA), Nafion (NF) 117 solution, and chitosan (CS) were purchased from Sigma-Aldrich, whereas glucose, citric acid, disodium hydrogen phosphate (Na_2HPO_4), sodium dihydrogen phosphate (NaH_2PO_4), ethanol, and acetone were bought from Chongqing Chuandong Chemical (Group) Co., Ltd., China. $HAuCl_4{\cdot}4H_2O$ (AR), cetyltrimethylammonium bromide (CTAB), and sodium borohydride were purchased from Shanghai Chemical Reagent Co. (Shanghai, China). Both methyl parathion and malathion were used as received from Dr. Ehrenstorfer GmbH. Graphene nanosheets (GNs) were acquired from Nanjing Xianfeng Nanomaterials Co. (China). All aqueous solutions were freshly prepared with deionized (DI) water (18 MΩ·cm) generated by a Millipore water system.

Preparation of the Biosensor. *Preparation of Plant Esterase, AuNPs, and GNs Suspension.* Crude plant esterase was first extracted from a 1:5 (w/w) mixed solution of wheat flour in DI water by using a centrifuge at 4000 rpm for 10 min at 4 °C, and then the purified plant esterase was prepared following a procedure reported by Yang et al.[10] Briefly, the crude plant esterase was further purified with a PEG1000/NaH_2PO_4 aqueous two-phase system by two-step extraction followed by 48 h of dialysis; then it was freeze-dried at −50 °C and ready for use. The gold nanoparticles (AuNPs) were freshly prepared following a seed-mediated growth method, in which CTAB was used as a stabilizer coated on the AuNP surfaces.[35,36] Then the reddish AuNP solution was collected and stored at 4 °C for subsequent experiments. To obtain homogeneous GNs suspension for subsequent use, 2 mg/mL GNs was sonicated in DI water for 30 min.

Preparation of the PLaE-CS/AuNPs-GNs/GCE. The PLaE-CS/AuNPs-GNs modified electrodes were prepared as follows: Before the modification of electrodes, glassy carbon electrodes (GCE, diameter = 3 mm) were polished carefully with 1 and 0.05 μm alumina slurries and sonicated for 1 min in acetone, ethanol, and DI water in sequence to remove any alumina residue on the electrode surface. After drying in air, 10 μL of GNs (2 mg/mL) and AuNPs (6.25 nM) mixtures with different volume ratios of GNs and AuNPs suspensions were directly drop-cast on the surface of the GCE, followed by full drying at room temperature. Then 4 μL of PLaE-CS (0.2% CS) (v/v = 2:1) solution was further cast on the surface of the electrode. After drying at 4 °C for 2 h, the modified electrodes were washed with 0.1 M, pH 6.5, PBS buffer to remove unbound PlaE. Finally, 10 μL of Nafion (NF) solution (0.1 wt % in 0.1 M pH 6.5 PBS buffer) was loaded on the modified GCE for serving as an entrapment and protective layer. The as-prepared electrode is denoted PLaE-CS/AuNPs-GNs/GCE. To elucidate the role of individual components in electrochemical biosensing, three control electrodes including PLaE-CS/GCE, PLaE-CS/GNs/GCE, and PLaE-CS/AuNPs/GCE were also prepared in a similar way.

Characterization and Electrochemical Measurements. Sodium dodecyl sulfate−polyacrylamide gel electrophoresis (SDS-PAGE) was carried out to confirm the purity of the plant esterase by following Deutscher's method.[37] A Lambda-900 UV−vis spectrophotometer (PerkinElmer) was used to measure the UV−vis absorption spectrum of AuNPs in aqueous solution. The microstructure and morphologic analyses of samples were characterized by a FEI Nova 400 field-emission scanning electron microscope (FESEM) and transmission electron microscopy (TEM) (Zeiss LIBRA 200, 200kV). Cyclic voltammetry (CV) and differential pulse voltammetry (DPV) measurements were performed with a CHI 660D Electrochemical Workstation (CH Instrument, USA) in a conventional three-electrode system. Ag/AgCl (3 M KCl) electrode and Pt wire were used as the reference and the auxiliary electrodes, respectively. All of the measurements were triplicated and recorded at room temperature.[15] In a typical DPV experiment, the biosensor was incubated in OPs solution for 10 min, and then the biosensor was submerged into substrate solution for 5 min followed by DPV recording. All experiments are conducted at the optimal temperature of PLaE, which is 30 °C.[14]

RESULTS AND DISCUSSION

Purification of Plant Esterase. Figure 1A shows the purified plant esterase in white powder after freeze-drying. As

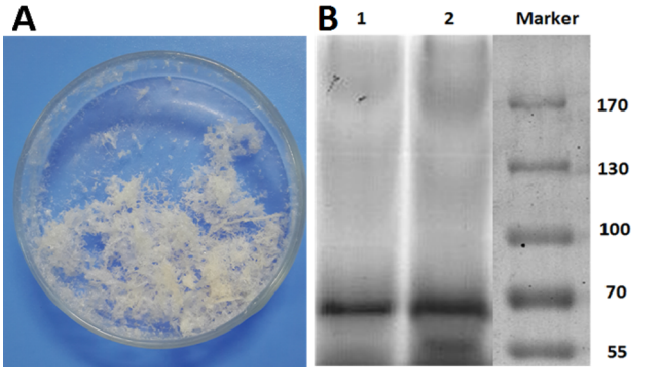

Figure 1. (A) Purified plant esterase in powder form; (B) SDS-PAGE of plant esterase (lanes: 1, plant esterase after the two-step extraction; 2, crude extract of plant esterase).

shown in the SDS-PAGE gel analysis (Figure 1B), two-step extraction using a PEG1000/NaH_2PO_4 aqueous two-phase system can significantly improve the purity of the as-prepared plant esterase (lane 1 vs lane 2). The molecular weight of the purified plant esterase was measured to be about 68 kDa, which is in good agreement with the reported value.[10] Such a simple

DOI: 10.1021/acs.jafc.5b03971
J. Agric. Food Chem. XXXX, XXX, XXX−XXX

purification protocol of plant esterase from plant allows mass production of plant esterase at low cost.

Characterization of the As-Prepared PLaE-CS/AuNPs-GNs Hybrid Composite. The as-prepared AuNPs solution displayed a light red color (inset of Figure S1). Its UV−vis absorption spectrum was further recorded and is shown in Figure S1. According to a literature report,[38,39] the size and concentration of AuNPs in the range of 5−100 nm can be estimated using the highest absorption peak wavelength. According to Figure S1, the absorption peak of AuNPs at 520 nm wavelength is 0.686; therefore, the estimated Au NPs have an average diameter of 13 ± 2 nm and a concentration of 6.25 nM,[36] which could be synthesized in high quality with good reproducibility.

The morphology of the nanocomposites was studied by SEM and TEM, as shown in Figure 2. Panels A and B of Figure 2

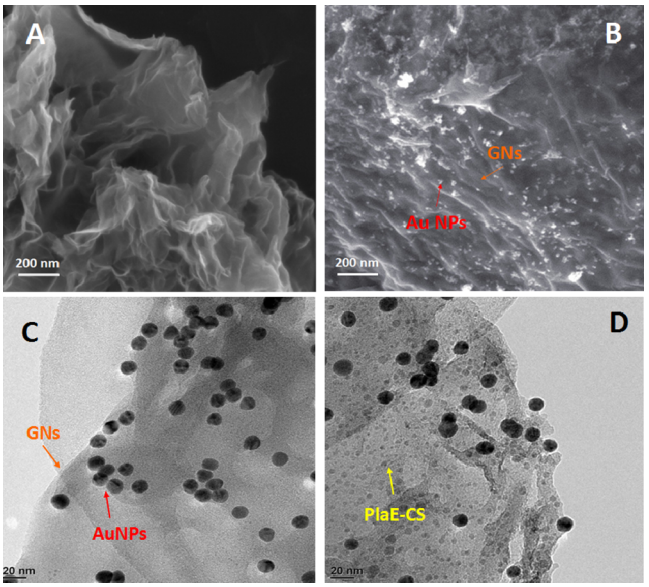

Figure 2. (A) SEM image of the GNs; (B) typical SEM image of AuNPs-GNs hybrid composite; (C, D) TEM images of AuNPs-GNs and PLaE-CS/AuNPs-GNs hybrid composite, respectively.

show the SEM images of the GNs and AuNPs-GNs, respectively. The crumpled GNs are observed due to its thin and large sheet-like morphology, whereas the AuNPs are uniformly adsorbed on the GNs surface. Such a AuNPs-GNs composite can provide biocompatible microenvironment to immobilized enzymes and also promote electron transfer during electrochemical reaction. The TEM image of AuNPs-GNs in Figure 2C also clearly indicates that the AuNPs possess an average diameter of 13 nm, in good agreement with results calculated from the UV−vis spectrum. Figure 2D shows the TEM image of PLaE-CS/AuNPs-GNs hybrid composite, in which plant esterase (PLaE) and chitosan (CS) composite particles have been clearly observed on the AuNPs-GNs composites. All of these results jointly demonstrate the successful preparation of PLaE-CS/AuNPs-GNs hybrid composite, which could be employed as an excellent biosensing platform for OPs detection.

Electrochemical Behavior of the As-Prepared Biosensors. The electrochemical behavior of plant esterase in 0.1 M, pH 6.5, PBS buffer solution in the presence or absence of 0.5 mM 1-NA was first investigated by CV scanning from −1.0 to 1.0 V (vs Ag/AgCl). Plant esterase belongs to the carboxylesterases, which can hydrolyze the carboxylic ester compounds.[40,41] As shown in Figure 3A, there is an obvious peak at +0.55 V in the presence of 0.5 mM 1-NA that can be attributed to the electrochemical oxidation of 1-naphthol, which is electroactive and the hydrolysis product of 1-NA by plant esterase (Scheme 1).

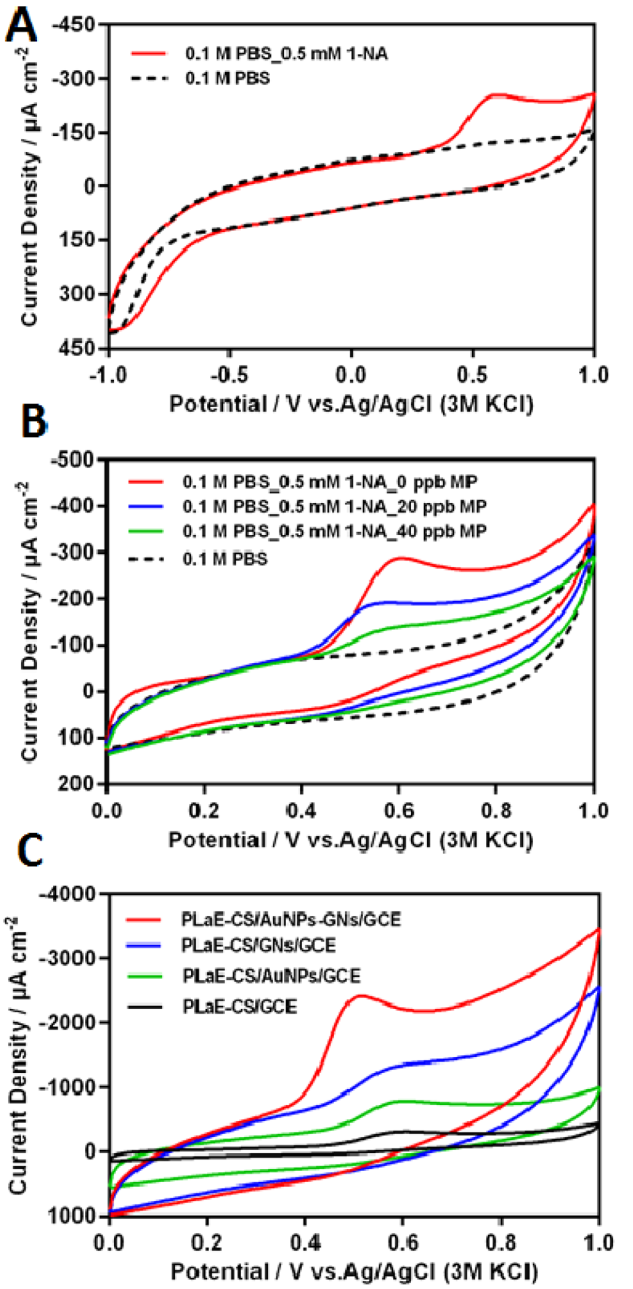

Figure 3. (A) Cyclic voltammograms of the PLaE-CS/GCE in 0.1 M, pH 6.5, PBS in the presence and absence of 0.5 mM 1-naphthyl acetate; (B) vyclic voltammograms of the PLaE-CS/GCE in 0.1 M, pH 6.5, PBS containing 0.5 mM 1-naphthyl acetate with different methyl parathion concentration (0, 20, and 40 ppb, respectively); (C) cyclic voltammograms of the PLaE-CS/AuNPs-GNs/GCE and three control electrodes (PLaE-CS/GCE, PLaE-CS/AuNPs/GCE, and PLaE-CS/GNs/GCE) in 0.1 M, pH 6.5, PBS containing 0.5 mM 1-naphthyl acetate. The scan rate was 0.10 V/s.

DOI: 10.1021/acs.jafc.5b03971
J. Agric. Food Chem. XXXX, XXX, XXX−XXX

Scheme 1. Reaction Scheme for the Plant Esterase Catalyzed Hydrolysis of 1-Naphthyl Acetate

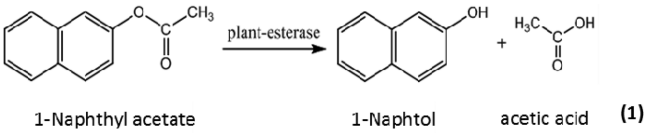

(1)

Figure 3B depicts the effect of different methyl parathion concentrations (0, 20, and 40 ppb) on CV behavior of the PLaE-CS/GCE in 0.1 M, pH 6.5, PBS containing 0.5 mM 1-NA. The oxidation peak current density at +0.55 V decreased with the increase of methyl parathion concentration, indicating that the presence of the methyl parathion inhibits the hydrolysis reaction of 1-NA by plant esterase (eq 1), resulting in the formation of a lesser amount of electroactive product (1-naphtol). This result also suggests that the detection of organophosphorus pesticides can be realized through plant esterase activity inhibition. To enhance the electrochemical signal, CVs of 1-naphthol (the hydrolysis product of 1-NA by plant esterase) were systematically investigated on four different biosensors: PLaE-CS/GCE, PLaE-CS/AuNPs/GCE, PLaE-CS/GNs/GCE, and PLaE-CS/AuNPs-GNs/GCE. As shown in Figure 3C, the PLaE-CS/AuNPs-GNs/GCE biosensor possesses the highest oxidation peak current and the lowest peak potential among all tested electrodes; therefore, it was used for subsequent experiments. This result demonstrated that AuNPs-GNs exhibit excellent conductivity in improving electron transfer, which was probably due to the good conductivity and adsorptive character of GNs and the good biocompatibility of AuNPs to preserve effectively the activity of the plant esterase during electrode preparation.[38,39] In addition, the AuNPs-GNs composites also provide a large number of active sites for protein binding, which probably act as rigid frame structure to retain the bioactivity of plant esterase before its inhibition by organophosphorus pesticides.

Optimization of the PLaE-CS/AuNPs-GNs Biosensor. To further optimize the developed OPs biosensor for quantification of the pesticides, optimization of the buffer pH, the ratio of AuNPs to GNs, the loading of AuNPs-GNs, and the amount of immobilized PLaE were determined to optimize the biosensor signal, and the corresponding results are presented in Figures S2−S5. To optimize each parameter, all other parameters are operated under their optimal conditions.

As shown in Figure S2, the bioactivity of the immobilized PLaE depends on the pH value of the 0.1 M PBS solution in the presence of 0.5 mM 1-NA. In the range from pH 5.0 to 8.0, the normalized signal initially increased with the pH value and then reached the maximum value at 6.5. Further increase of pH values resulted in the decrease of the electrochemical response. Therefore, a 0.1 M, pH 6.5, PBS buffer solution was used in subsequent experiments. Moreover, a ratio (v/v) of GNs (2 mg/mL) to AuNPs (6.5 nM) of 2:1 with a total loading of 10 μL shows the highest normalized signal, which was demonstrated in Figures S3 and S4. The amount of PLaE immobilized on the biosensor was another important factor affecting biosensor performance, which was also optimized. As shown in Figure S5, with the increase of PLaE from 0.14 to 0.38 U, the normalized signal of the biosensor increased initially and then reached a maximum at 0.26 U. Further increase of the

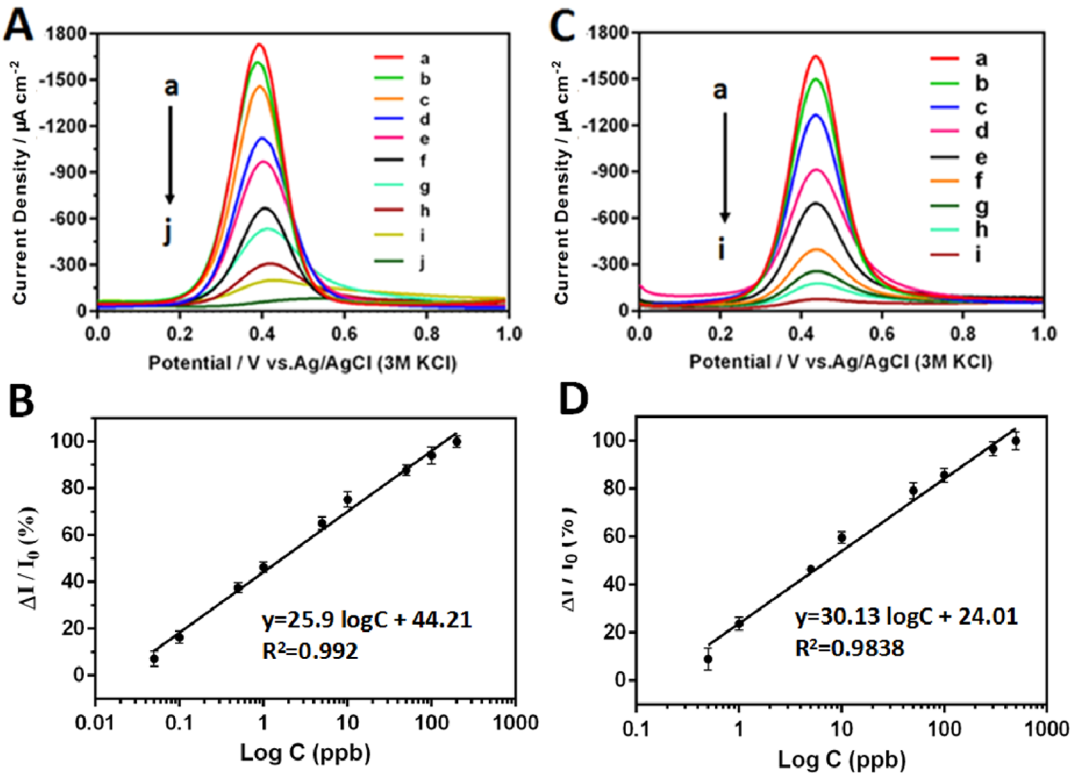

Figure 4. (A, C) DPVs on the PLaE-CS/AuNPs-GNs/GCE in 0.1 M, pH 6.5, PBS containing 0.5 mM 1-naphthyl acetate with different concentrations of methyl parathion (from top to bottom: 0, 0.05, 0.1, 0.5, 1, 5, 10, 50, 100, and 200 ppb, respectively) and different concentrations of malathion (from top to bottom: 0, 0.5, 1, 5, 10, 50, 100, 300, and 500 ppb, respectively); (B, D) corresponding calibration curves of (A) and (C) ($\Delta I/I_0$ vs log C).

DOI: 10.1021/acs.jafc.5b03971
J. Agric. Food Chem. XXXX, XXX, XXX−XXX

Table 1. Comparison of the PLaE-Based Biosensor in This Study with Other Reported AChE-Based Biosensors for Methyl Parathion and Malathion Detection

pesticide	electrode	linear range	detection limit (nM)	ref
methyl parathion	AChE-LDHs/GCE	19−1100 nM 1.1−15 μM	2.3	42
	PANI/CNT wrapped with ssDNA/Au	0.011−1000 nM	0.001	43
	AChE-nano$CaCO_3$-chi/GCE	18−759 nM 2.84−14.24 μM	3.8	44
	AChE-AuNPs-PPy/GCE	18−450 nM 1.89−17 μM	7.5	25
	AChE-SF/MWNTs/GCE	3.5−2000 μM	500	45
	PLaE-CS/AuNPs-GNs/GCE	0.19−760 nM	0.19	present
malathion	AChE-ZrO_2/CHIT composite film/GCE	10−590 nM	5.0	19
	AChE-CHIT-GNPs/Au	3−300 nM 6−60 μM	3.0	46
	AChE-AuNPs-$CaCO_3$/silica sol-gel/AuE	0.1−100 nM	0.1	27
	AChE-Fe_3O_4NP/MWCNTs/ITO	0.1−70 nM	0.1	47
	AChE/AuNPs/MWCNTs	3−3027 nM 6.6−44 μM	1.8	28
	PLaE-CS/AuNPs-GNs/GCE	1.5−1513.5 nM	1.51	present

amount of PLaE led to a slight decrease of the normalized signal, which can be attributed to the increased mass transfer resistance and inaccessibility of PLaE embedded in the deeper layer. Thus, 0.26 U PLaE was used for subsequent experiments.

Effect of Substrate Concentration, Reaction Time (with Substrate), and Incubation Time (with OPs for Inhibition) on the Sensing Performance of PLaE-CS/AuNPs-GNs Biosensor. Before its application for the detection of pesticides, the effects of substrate concentration, reaction time (with substrate), and incubation time (with OPs for inhibition) on the sensing performance of PLaE-CS/AuNPs-GNs were also optimized to maximize the signal. As shown in Figure S6, the signal initially increases with the concentration of 1-NA linearly; however, when 1-NA concentration reaches 0.5 mM, further increase of 1-NA concentration does not improve the signal due to the fact that the substrate is excessive compared to the immobilized PLaE. The reaction time is also optimized under the optimal substrate concentration of 0.5 mM. As expected, with the increase of reaction time, the signal increased initially (Figure S7). After 5 min of reaction time, the signal leveled off. Therefore, 5 min of reaction time with substrate was selected for subsequent experiments. Furthermore, the activity of the enzyme due to OPs inhibition was affected by the incubation time of PLaE with pesticides. Therefore, the incubation time of biosensor with pesticides is also optimized. Figure S8 exhibits the effect of incubation time of biosensor with 10 ppb of methyl parathion on the observed signal. One can see that the normalized signal increases rapidly with incubation time and then levels off after 10 min, indicating that the binding interaction between pesticides and PLaE reaches saturation. Thus, 10 min was selected as the optimum incubation time in the following detection.

Detection of Methyl Parathion and Malathion. After incubation with different concentrations of methyl parathion and malathion, differential pulse voltammetry (DPV) was used to evaluate the sensitivity of the biosensor under the optimized operating conditions. Panels A and C of Figure 4 show the DPV results, whereas panels B and D display the corresponding semilogarithmic calibration curves of inhibition percentage ($\Delta I/I_0$) versus logarithmic of pesticides concentration (log C) (semilog line: X-axis is logarithmic, Y-axis is linear). The linear equations are $\Delta I/I_0$ (%) = 25.9 log C + 44.21 (R^2 = 0.992) from 0.05 to 200 ppb (0.19−760 nM) and $\Delta I/I_0$ (%) = 30.13 log C + 24.01 (R^2 = 0.9838) from 0.5 to 500 ppb (1.51−1513.5 nM) for methyl parathion and malathion, respectively, in which I_0 represents the peak current with 0 ppb of pesticides by DPV, whereas ΔI presents the D value of peak current between I_0 and the one in the presence of pesticides. The limits of detection for methyl parathion and malathion were 50 ppt (0.19 nM) and 0.5 ppb (1.51 nM) (S/N = 3), respectively. Compared with AChE-based OPs biosensors reported in the literature (Table 1), both the detection ranges and the detection limits obtained in the present work were better than or on par with the results from those AChE biosensors. Such excellent biosensing performance might be attributed to the synergistic effect of several contributions: (1) PLaE can be inhibited by OPs sensitively; (2) AuNPs-GNs increase the surface area to allow monolayered immobilize of PLaE-CS (supported by TEM image in Figure 2D) and also enhance the electron transfer, thus enhancing the biosensing performance; and (3) CS provides a favorable microenvironment for PLaE. Notably, the plant esterase can be purified in large scale at significantly lower cost compared to AChE. Therefore, PlaE-based OPs biosensor opens a new avenue in the development of ultrasensitive and cost-effective OPs biosensor.

Interference Study. To further demonstrate the specificity of the as-prepared PLaE-CS/AuNPs-GNs/GCE biosensor for OPs detection, the potential interference due to the presence of some common interfering species in samples was investigated (Figure 5), including non-organophosphate pesticides, metal ions, oxygen-containing inorganic ions, glucose, and citric acid.[48] The current response was normalized on the basis of the response under optimized conditions for 10 ppb of methyl parathion.

Figure 5 presents that the normalized signal for 10 ppb of methyl parathion (100%, Figure 5a) was compared with the normalized signal obtained in the coexistence of different interfering species (Figure 5b−m). The results showed that no significant changes in the signals were detected for the

DOI: 10.1021/acs.jafc.5b03971
J. Agric. Food Chem. XXXX, XXX, XXX−XXX

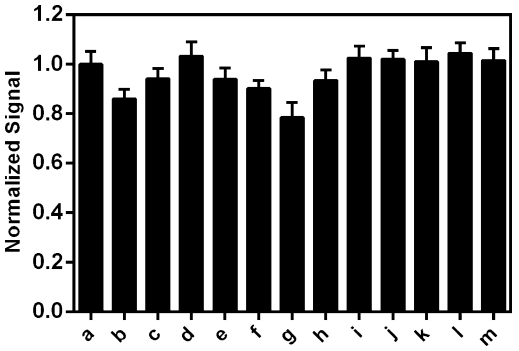

Figure 5. DPVs on the PLaE-CS/AuNPs-GNs/GCE with 0.1 M, pH 6.5, PBS containing 0.5 mM 1-napthyl acetate in the presence of 10 ppb of methyl parathion (a) and 10 ppb of methyl parathion with coexistence of 10 ppb of carbendazin (b), 10 ppb of lindane (c), 1 ppm of Fe^{3+} (d), 1 ppm of Zn^{2+} (e), 1 ppm of Cu^{2+} (f), 1 ppm of Pb^{2+} (g), 1 ppm of K^{+} (h), 1 ppm of NO_3^{-} (i), 1 ppm of PO_4^{3-} (j), 1 ppm of SO_4^{2-} (k), 0.5 mM glucose (l), or 0.5 mM citric acid (m), respectively.

coexistence of 10 ppb of lindane (c), 1 ppm of Fe^{3+} (d), 1 ppm of Zn^{2+} (e), 1 ppm of Cu^{2+} (f), 1 ppm of K^{+} (h), 1 ppm of NO_3^{-} (i), 1 ppm of PO_4^{3-} (j), 1 ppm of SO_4^{2-} (k), 0.5 mM glucose (l), or 0.5 mM citric acid (m) after co-incubation with 10 ppb of methyl parathion at the optimized conditions. However, the addition of 10 ppb of carbendazin (b) and 1 ppm of Pb^{2+} (g) to 10 ppb of methyl parathion interfered with the detection to certain degrees (85.97 and 78.37%, respectively), which might be attributed to the fact that the inhibition of plant esterase activity by toxic compounds lacks specificity, which is also typical for other AChE-based biosensors.[15] The storage stability of the PlaE-CS/AuNPs-GNs biosensor was also studied by measuring its response to 1-NA and storing it in 0.1 M, pH 6.5, PBS buffer at 4 °C when it was not in use. There was no obvious decrease in the normalized signal to 0.5 mM 1-NA for a period of 9 days, and the biosensor also retained 73% of its initial signal after 15 days, indicating the acceptable stability of PLaE-based biosensor.

Analysis of Real Samples. To further illustrate the practical applications of the developed OPs biosensor, the PLaE-CS/AuNPs-GNs/GCE electrode is applied for the determination of methyl parathion and malathion in smashed carrot and apple samples by a standard spike recovery test. Notably, the smashed sample solution was centrifuged at 37 °C for 20 min at 8000 rpm, and then the supernatant was filtered through a well-defined 0.2 μm PVDF filter and diluted 10 times with DI water. In addition, the pH and ionic strength of the sample solution were adjusted to match with the PBS buffer used in this experiment. After sample pretreatment, different concentrations of methyl parathion and malathion were spiked into the samples, and then the developed biosensor was employed to detect the spiked OPs concentration. Table 2 shows that the recoveries of spiked methyl parathion and malathion in carrot and apple samples were observed in the range from 92.0 ± 3.85 to 109.5 ± 5.26%. Such good recovery rates with the low relative standard deviations for methyl parathion and malathion indicate that the developed OPs biosensor based on PLaE-CS/AuNPs-GNs nanocomposites was highly precise and reliable in the real sample analysis.

Conclusion. In the present work, a new PLaE-CS/AuNps-GNs biosensor was successfully constructed and its application for ultrasensitive and selective detection of organophosphate

Table 2. Recovery Studies of Spiked Methyl Parathion and Malathion in Carrots and Apples (Each Result Was the Average of Three Determinations)

sample	pesticide	added (ppb)	found (ppb)	recovery (%)	RSD (%)
carrot	methyl parathion	0.50	0.46	92.00	3.85
		5.00	5.37	107.40	4.32
		10.00	10.33	103.30	5.01
	malathion	1	0.93	93.00	4.62
		5.00	5.26	105.20	3.89
		10.00	9.40	94.00	4.37
apple	methyl parathion	0.50	0.52	104.00	3.29
		5.00	4.91	98.20	4.51
		10.00	10.26	102.60	5.12
	malathion	1	1.10	109.50	5.26
		5.00	4.89	97.80	3.12
		10.00	10.49	104.90	4.25

pesticides was demonstrated. PLaE was purified from plants and then used as an alternative for expensive AChE without sacrifice of the biosensing performance. The as-prepared biosensor was also systematically optimized with respect to the loading of PLaE, GNs, and AuNPs, the operating pH, or the reaction time as well as the incubation time. The PLaE-CS/AuNPs-GNs/GCE biosensor showed wide detection ranges with limits of detection as low as 50 ppt (0.19 nM) and 0.5 ppb (1.51 nM) for methyl parathion and malathion, respectively. Such excellent biosensing performance can be attributed to enhanced surface area, fast electron transfer, good electrical conductivity, and desirable biocompatibility. Finally, the detection of spiked methyl parathion and malathion in carrots and apples was demonstrated with excellent recovery rates using the developed biosensor. These results indicate that the PLaE-CS/AuNPs-GNs nanocomposite is a promising candidate in the development of a biosensor for organophosphorus pesticides with high performance.

■ ASSOCIATED CONTENT

Ⓢ Supporting Information

The Supporting Information is available free of charge on the ACS Publications website at DOI: 10.1021/acs.jafc.5b03971.

UV−vis absorbance spectrum of the AuNPs; effect of pH, loading of GNs-Au NPs, GNs/Au NPs ratio, loading of plant esterase, 1-naphthyl acetate concentration, reaction time, and incubation time on the response of the PLaE-CS/AuNPs-GNs/GCE biosensor in 0.1 M PBS buffer solution (PDF)

■ AUTHOR INFORMATION

Corresponding Authors

*(C.J. Hou) E-mail: houcj@cqu.edu.cn. Phone: +86 23 6511 1022. Fax: +86 23 6510 2507.

*(Y. Lei) E-mail: ylei@engr.uconn.edu. Phone: +1 860 486 4554. Fax: +1 860 486 2959.

Funding

The present study was financially supported by the Natural Science Foundation of China (31171684), Key Technologies R&D Program of China (2014BAD07B02), Key Technologies R&D Program of Sichuan Province of China (2013FZ0043),

DOI: 10.1021/acs.jafc.5b03971
J. Agric. Food Chem. XXXX, XXX, XXX−XXX

Open Fund of Liquor-Making Biotech and Application Key Laboratory of Sichuan Province (NJ2014-03), Chongqing's Postgraduate Research Innovation Projects (CYB14028), and the Short-term International Academic Fund of Chongqing University 2014 Overseas Visiting Student Project Agreement. We are grateful for the support from the sharing fund of Chongqing university's large equipment.

Notes

The authors declare no competing financial interest.

REFERENCES

(1) Liu, R. H.; Yang, C.; Xu, Y. M.; Xu, P.; Jiang, H.; Qiao, C. L. Development of a whole-cell biocatalyst/biosensor by display of multiple heterologous proteins on the *Escherichia coli* cell surface for the detoxification and detection of organophosphates. *J. Agric. Food Chem.* **2013**, *61*, 7810−7816.

(2) Singh, B. K. Organophosphorus-degrading bacteria: ecology and industrial applications. *Nat. Rev. Microbiol.* **2009**, *7*, 156−164.

(3) Gong, J. M.; Miao, X. J.; Zhou, T.; Zhang, L. Z. An enzymeless organophosphate pesticide sensor using Au nanoparticle-decorated graphene hybrid nanosheet as solid-phase extraction. *Talanta* **2011**, *85*, 1344−1349.

(4) Pundir, C. S.; Chauhan, N. Acetylcholinesterase inhibition-based biosensors for pesticide determination: a review. *Anal. Biochem.* **2012**, *429*, 19−31.

(5) Mulchandani, A.; Rajesh. Microbial biosensors for organophosphate pesticides. *Appl. Biochem. Biotechnol.* **2011**, *165*, 687−699.

(6) Chapalamadugu, S.; Chaudhry, G. S. Microbiological and biotechnological aspects of metabolism of carbamates and organophosphates. *Crit. Rev. Biotechnol.* **1992**, *12*, 357−389.

(7) Wang, M.; Gu, X.; Zhang, G.; Zhang, D.; Zhu, D. Continuous colorimetric assay for acetylcholinesterase and inhibitor screening with gold nanoparticles. *Langmuir* **2009**, *25*, 2504−2507.

(8) Zhou, Q.; Yang, L.; Wang, G. C.; Yang, Y. Acetylcholinesterase biosensor based on SnO_2 nanoparticles-carboxylic graphemenafion modified electrode for detection of pesticides. *Biosens. Bioelectron.* **2013**, *49*, 25−31.

(9) Wong, F. C. M; Ahmad, M.; Heng, L. Y.; Peng, L. B. An optical biosensor for dichlovos using stacked sol−gel films containing acetylcholinesterase and a lipophilic chromoionophore. *Talanta* **2006**, *69*, 888−893.

(10) Yang, L. M.; Huo, D. Q.; Hou, C. J.; He, K.; Lv, F. J.; Fa, H. B.; Luo, X. G. Purification of plant-esterase in PEG1000/NaH_2PO_4 aqueoustwo-phase system by a two-step extraction. *Process Biochem.* **2010**, *45*, 1664−1671.

(11) Cummins, I.; Burnet, M.; Edwards, R. Biochemical characterisation of esterases active in hydrolysing xenobiotics in wheat and competing weeds. *Physiol. Plant.* **2001**, *113*, 477−485.

(12) Cummins, I.; Edwards, R. Purification and cloning of an esterase from the weed black-grass (*Alopecurus myosuroides*), which bioactivates aryloxyphenoxypropionate herbicides. *Plant J.* **2004**, *39*, 894−904.

(13) Huo, D. Q.; Yang, L. M.; Hou, C. J. Optical detection of dimethyl methyl-phosphonate with monosulfonate tetraphenyl porphyrin-plant-esterase complex. *Sens. Lett.* **2009**, *7*, 72−78.

(14) Li, J. K.; Zhou, Y. L.; Wen, Y. X.; Wang, J. H.; Hu, Q. H. Studies on the purification and characterization of soybean esterase, and its sensitivity to organophosphate and carbamate pesticides. *Agric. Sci. China* **2009**, *8*, 455−463.

(15) Hou, C. J.; He, K.; Yang, L. M.; Huo, D. Q.; Yang, M. Catalytic characteristics of plant-esterase from wheat flour. *World J. Microbiol. Biotechnol.* **2012**, *28*, 541−548.

(16) Jha, N.; Ramaprabhu, S. Development of Au nanoparticles dispersed carbon nanotube-based biosensor for the detection of paraoxon. *Nanoscale* **2010**, *2*, 806−810.

(17) Wu, S.; Lan, X.; Zhao, W.; Li, Y.; Zhang, L.; Wang, H.; Han, M.; Tao, S. Controlled immobilization of acetylcholinesterase on improved hydrophobic gold nanoparticle/Prussian blue modified surface for ultra-trace organophosphate pesticide detection. *Biosens. Bioelectron.* **2011**, *27*, 82−87.

(18) Du, D.; Wang, M.; Cai, J.; Qin, Y.; Zhang, A. One-step synthesis of multiwalled carbon nanotubes−gold nanocomposites for fabricating amperometric acetylcholinesterase biosensor. *Sens. Actuators, B* **2010**, *143*, 524−529.

(19) Yang, Y.; Guo, M.; Yang, M.; Wang, Z.; Shen, G.; Yu, R. Determination of pesticides in vegetable samples using an acetylcholinesterase biosensor based on nanoparticles ZrO_2/chitosan composite film. *Int. J. Environ. Anal. Chem.* **2005**, *85*, 163−175.

(20) Wang, K.; Li, H. N.; Wu, J.; Ju, C.; Yan, J. J.; Liu, Q.; Qiu, B. TiO_2-decorated graphene nanohybrids for fabricating an amperometric acetylcholinesterase biosensor. *Analyst* **2011**, *136*, 3349−3354.

(21) Wang, K.; Liu, Q.; Dai, L.; Yan, J.; Ju, C.; Qiu, B.; Wu, X. A highly sensitive and rapid organophosphate biosensor based on enhancement of CdS-decorated graphene nanocomposite. *Anal. Chim. Acta* **2011**, *695*, 84−88.

(22) Saha, k.; Agasti, S. S.; Kim, C. K.; Li, X. N.; Rotello, V. M. Gold nanoparticles in chemical and biological sensing. *Chem. Rev.* **2012**, *112*, 2739−2779.

(23) Wei, M.; Zeng, G. Y.; Lu, Q. Y. Determination of organophosphate pesticides using an acetylcholinesterase-based biosensor based on a boron-doped diamond electrode modified with gold nanoparticles and carbon spheres. *Microchim. Acta* **2014**, *181*, 121−127.

(24) Cao, X. D.; Ye, Y. K.; Liu, S. Q. Gold nanoparticle-based signal amplification for biosensing. *Anal. Biochem.* **2011**, *417*, 1−16.

(25) Gong, J.; Wang, L.; Zhang, L. Electrochemical biosensing of methyl parathion pesticide based on acetylcholinesterase immobilized onto Au−polypyrrole interlaced network-like nanocomposite. *Biosens. Bioelectron.* **2009**, *24*, 2285−2288.

(26) Buiculescu, R.; Chaniotakis, N. A. The stabilization of Au NP-AChE nanocomposites by biosilica encapsulation for the development of a thiocholine biosensor. *Bioelectrochemistry* **2012**, *86*, 72−77.

(27) Chauhan, N. H.; Narang, N.; Pundir, C. S. Immobilization of rat brain acetylcholinesterase on porous gold-nanoparticle−$CaCO_3$ hybrid material modified Au electrode for detection of organophosphorous insecticides. *Int. J. Biol. Macromol.* **2011**, *49*, 923−929.

(28) Allen, M. J.; Tung, V. C.; Kaner, R. B. Honeycomb carbon: a review of graphene. *Chem. Rev.* **2010**, *110*, 132−145.

(29) Gong, J. M.; Miao, X. G.; Zhou, T.; Zhang, L. Z. An enzymeless organophosphate pesticide sensor using Au nanoparticle-decorated graphene hybrid nanosheet as solid-phase extraction. *Talanta* **2011**, *85*, 1344−1349.

(30) Kuila, T.; Bose, S.; Khanra, P.; Mishra, A. K.; Kim, N. H.; Lee, J. H. Recent advances in graphene-based biosensors. *Biosens. Bioelectron.* **2011**, *26*, 4637−4648.

(31) Oliveira, T. M. B. F.; Barroso, M. F.; Morais, S. Sensitive bi-enzymatic biosensor based on polyphenoloxidases−gold nanoparticles−chitosan hybrid film−graphene doped carbon paste electrode for carbamates detection. *Bioelectrochemistry* **2014**, *98*, 20−29.

(32) Prakash, S.; Chakrabarty, T.; Singh, A. K.; Shahi, V. K. Polymer thin films embedded with metal nanoparticles for electrochemical biosensors applications. *Biosens. Bioelectron.* **2013**, *41*, 43−53.

(33) Norouzi, P.; Pirali-Hamedani, M.; Ganjali, M. R.; Faridbod, F. A. A novel acetyl cholinesterase biosensor based on chitosan−gold nanoparticles film for determination of monocrotophos using FFT continuous cyclic voltammetry. *Int. J. Electrochem. Sci.* **2010**, *5*, 1434−1446.

(34) Zhai, C.; Xia, S.; Zhao, W.; Gong, Z.; Wang, X. Acetylcholinesterase biosensor based on chitosan/Prussian blue/multiwall carbon nanotubes/hollowgold nanospheres nanocomposite film by one-step electrodeposition. *Biosens. Bioelectron.* **2013**, *42*, 124−130.

(35) Sau, T. K.; Murphy, C. J. Room temperature, high-yield synthesis of multiple shapes of gold nanoparticles in aqueous solution. *J. Am. Chem. Soc.* **2004**, *126*, 8648−8649.

DOI: 10.1021/acs.jafc.5b03971
J. Agric. Food Chem. XXXX, XXX, XXX−XXX

(36) Orendorff, C. J.; Murphy, C. J. Quantitation of metal content in the silver-assisted growth of gold nanorods. *J. Phys. Chem. B* **2006**, *110*, 3990−3994.
(37) Deutscher, M., Ed. Electrophoretic methods. *Guide to Protein Purification, Methods in Enzymology*; Academic Press: New York, 1990; Vol. 182, pp 425−488
(38) Li, C. M.; Zhen, S. J.; Wang, J.; Li, Y. F.; Huang, C. Z. A gold nanoparticles-based colorimetricassay for alkaline phosphatase detection with tunable dynamic range. *Biosens. Bioelectron.* **2013**, *43*, 366−371.
(39) Liu, H.; Su, X.; Duan, C. Y.; Dong, X. N.; Zhou, S. L.; Zhu, Z. F. Microwave-assisted hydrothermal synthesis of Au NPs−graphene composites for H_2O_2 detection. *J. Electroanal. Chem.* **2014**, *731*, 36−42.
(40) Wolfgang, J.; Krisch, K.; Conney, A. The carboxylesterases/amidases of mammalian liver and their possible significance. *Crit. Rev. Toxicol.* **1975**, *3*, 371−434.
(41) Satoh, T.; Hosokawa, M. Structure, function and regulation of carboxylesterases. *Chem.-Biol. Interact.* **2006**, *162*, 195−211.
(42) Gong, J. M.; Guan, Z. Q.; Song, D. Biosensor based on acetylcholinesterase immobilized onto layered double hydroxides for flow injection/amperometric detection of organophosphate pesticides. *Biosens. Bioelectron.* **2013**, *39*, 320−323.
(43) Viswanathan, S.; Radecka, H.; Radecka, J. Electrochemical biosensor for pesticides based on acetylcholinesterase immobilized on polyaniline deposited on vertically assembled carbon nanotubes wrapped with ssDNA. *Biosens. Bioelectron.* **2009**, *24*, 2772−2777.
(44) Gong, J. M.; Liu, T.; Song, D. D.; Zhang, X. B.; Zhang, L. Z. One-step fabrication of three-dimensional porous calcium carbonate−chitosan composite film as the immobilization matrix of acetylcholinesterase and its biosensing on pesticide. *Electrochem. Commun.* **2009**, *11*, 1873−1876.
(45) Xue, R.; Kang, T. F.; Lu, L. P.; Cheng, S. Y. Immobilization of acetylcholinesterase via biocompatible interface of silk fibroin for detection of organophosphate and carbamate pesticides. *Appl. Surf. Sci.* **2012**, *258*, 6040−6045.
(46) Du, D.; Ding, J. W.; Cai, J.; Zhang, A. D. One-step electrochemically deposited interface of chitosan−gold nanoparticles for acetylcholinesterase biosensor design. *J. Electroanal. Chem.* **2007**, *605*, 53−60.
(47) Chauhan, N. H.; Pundir, C. S. An amperometric acetylcholinesterase sensor based on Fe_3O_4 nanoparticle/multi-walled carbon nanotube-modified ITO-coated glass plate for the detection of pesticides. *Electrochim. Acta* **2012**, *67*, 79−86.
(48) Huo, D. Q.; Li, Q.; Zhang, Y. C.; Hou, C. J.; Lei, Y. A highly efficient organophosphorus pesticides sensor based on CuO nanowires-SWCNTs hybrid nanocomposite. *Sens. Actuators, B* **2014**, *199*, 410−417.

DOI: 10.1021/acs.jafc.5b03971
J. Agric. Food Chem. XXXX, XXX, XXX−XXX